A Review of Sliding Mode Observers Based on Equivalent Circuit Model for Battery SoC Estimation

Sui, Xin; He, Shan; Stroe, Daniel-Ioan; Huang, Xinrong; Jinhao, Meng; Teodorescu, Remus

Published in:
Proceedings of the 2019 IEEE 28th IEEE International Symposium on Industrial Electronics (ISIE)

DOI (link to publication from Publisher):
10.1109/ISIE.2019.8781412

Publication date:
2019

Document Version
Publisher's PDF, also known as Version of record

A review of sliding mode observers based on equivalent circuit model for battery SoC estimation

Xin Sui
Department of Energy Technology
Aalborg University
Aalborg, Denmark
xin@et.aau.dk

Shan He
Department of Energy Technology
Aalborg University
Aalborg, Denmark
she@et.aau.dk

Daniel-Ioan Stroe
Department of Energy Technology
Aalborg University
Aalborg, Denmark
dis@et.aau.dk

Xinrong Huang
Department of Energy Technology
Aalborg University
Aalborg, Denmark
hxi@et.aau.dk

Jinhao Meng
School of Automation
Northwestern Polytechnical University
Xi'an, China
scmjh2008@163.com

Remus Teodorescu
Department of Energy Technology
Aalborg University
Aalborg, Denmark
ret@et.aau.dk

***Abstract*—Battery technology is a major technical bottleneck with electric vehicles (EVs). It is necessary to perform state of charge (SoC) estimation in order to ensure battery safe usage and reduce its average lifecycle cost. Sliding mode observer (SMO) has been used widely in battery SoC estimation owing to its simplicity and robustness to both parameter variations and external disturbances. The SMO uses a switching function of the model error as feedback to drive estimated states to a hypersurface where there is no difference between measured and estimated output exactly. In this paper, three kinds of SMOs based on equivalent circuit model (ECM) for SoC estimation in the existing literatures are reviewed. Their difference in the structures and principles are discussed in the hope of providing some inspirations to the design of efficient SMO based SoC estimation methods.**

Keywords— battery, sliding mode observer, state of charge estimation, comparison

I. INTRODUCTION

Electric vehicles (EVs) have emerged as a viable environmentally friendly solution for global warming mitigation [1]. Battery as an important storage component in EVs has attracted more and more attention in the world. An effective battery management system (BMS) is compulsory so that battery can prevent any physical damages and handle cell unbalancing [2]. Among the various functions of a BMS, monitoring the SoC is critical in practical applications where it is necessary to determine how long the cell will last. This information is implemented in the BMS and is used to know when to stop charging and discharging, as over-charging or over-discharging may cause permanent internal damage [3].

Since batteries are complex electrochemical devices with a distinct nonlinear behavior depending on various internal and external conditions, their monitoring is a challenging task [4]. One of the most implemented methods is the Coulomb counting method. The necessity of an accurate initial SOC and the accumulation of the current measurement errors make the Coulomb counting method doubtful for a highly accurate SOC [5]. For open-circuit voltage estimation, a long time (up to hours) is needed for a battery to be relaxed to reach its equilibrium, which makes it merely suitable at the beginning or end of the entire process [6]. Another technique is the battery internal impedance measurement, which loads a series of small amplitude ac signals with a wide range of frequencies into the battery to detect the responses for internal impedance calculation. However, this is only suitable in lab research TABLE I. -[8]. The data-driven methods are based on artificial neural networks, support vector machine, extreme learning machine, and so on [9]-[12]. But the practicability of data-driven methods is closely related to the data samples and computing burden is high in the BMS.

Model-based methods have advantages of being insensitive to initial SOC, which seems to be a better tradeoff between accuracy and computing efficiency. Accordingly, Kalman filter [13], H-infinity filter [14], and particle filter [15] can achieve accurate SoC estimation. However, considering the performance of BMS when running the simulated algorithms, SMO is a good candidate in computational time, code complexity, and memory usage [16]. Because the ECM is easy to be established, the focus of this paper is the SMOs based on ECM. Three kinds of SMO methods including first-order constant-gain SMO, second-order constant-gain SMO and first-order adaptive gain SMO are reviewed. Their difference in structures and principles are discussed in order to provide a reference for designing SMO based SoC estimation methods.

II. BATTERY MODEL

Among these model-based SMOs, there are two main differences: one is the sliding mode term of the observer, the other one is the used model. Moreover, an accurate model is a prerequisite for the accurate SoC estimation. Therefore, in this section, two commonly used battery models including Randle circuit model (RCM) and RC circuit model (RCCM) are firstly introduced.

978-1-7281-3665-3/19/$31.00 ©2019 IEEE

A. Randle Circuit Model

Various ECMs have been proposed to capture the dynamic characteristics of batteries [17]. One of the prevailing battery models is the RCM [18] and its nth-order structure is shown in Fig. 1. V_{oc} is the open circuit voltage and it has a nonlinear function relationship with battery SoC represented by Z. R_0 is the internal ohmic resistance characterizing the electrolyte and interphase resistance of the battery. N parallel-connected networks consist of R_1, …, R_n and C_1, …, C_n which reflect the charge transfer and diffusion effect. I and V_t denote the battery's current and the terminal voltage, respectively. According to Fig. 1, the state equation of the nth-order RCM can be expressed as

$$\begin{bmatrix} \dot{V}_1 \\ \dot{V}_2 \\ \vdots \\ \dot{V}_n \\ \dot{V}_{oc} \end{bmatrix} = diag\begin{pmatrix} \frac{-1}{R_1C_1} & \frac{-1}{R_2C_2} & \cdots & \frac{-1}{R_nC_n} & 0 \end{pmatrix} \begin{bmatrix} V_1 \\ V_2 \\ \vdots \\ V_n \\ V_{oc} \end{bmatrix} + \begin{bmatrix} 1/C_1 \\ 1/C_2 \\ \vdots \\ 1/C_n \\ 1/Q_n \end{bmatrix} i_t + \begin{bmatrix} f_1 \\ f_2 \\ \vdots \\ f_n \\ f_{n+1} \end{bmatrix} \quad (1)$$

where Q_n is the battery capacity. The expression of the terminal voltage is given as

$$V_t = \begin{bmatrix} -1 & -1 & \cdots & -1 & 1 \end{bmatrix} \begin{bmatrix} V_1 \\ V_2 \\ \vdots \\ V_n \\ V_{oc} \end{bmatrix} - R_0 i_t \quad (2)$$

Considering the accuracy and the computational complexity, n always takes the value of 1 or 2. If the dimension of the circuit model is 1, the circuit model is the first-order RCM, and if the dimension is 2, it is the second-order RCM.

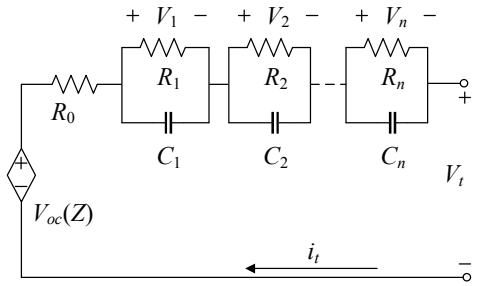

Fig. 1. Battery *nth*-order Randle circuit model.

B. RC Circuit Model

The structure of RCCM [19] is shown in Fig. 2, where R_e is the propagation resistor, C_p and R_p are the polarization capacitance and diffused resistor, V_p is the polarized voltage, R_0 is the ohmic resistance, I is the input current and V_t is the battery terminal voltage. The state equation of RCCM and output voltage can be expressed as

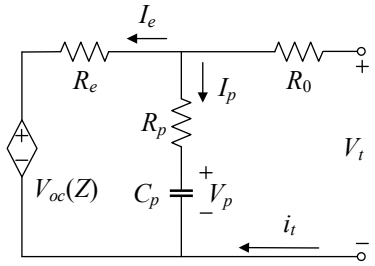

Fig. 2. Battery RC circuit model.

$$\begin{bmatrix} \dot{V}_p \\ \dot{V}_{oc} \end{bmatrix} = \begin{bmatrix} \frac{-1}{C_p(R_e+R_p)} & \frac{1}{C_p(R_e+R_p)} \\ \frac{1}{Q_n(R_e+R_p)} & \frac{-1}{Q_n(R_e+R_p)} \end{bmatrix} \begin{bmatrix} V_p \\ V_{oc} \end{bmatrix} + \begin{bmatrix} \frac{-R_e}{C_p(R_e+R_p)} \\ \frac{-R_e}{Q_n(R_e+R_p)} \end{bmatrix} i_t + \begin{bmatrix} f_1 \\ f_2 \end{bmatrix} \quad (3)$$

$$V_t = \begin{bmatrix} \frac{R_e}{R_e+R_p} & \frac{R_p}{R_e+R_p} \end{bmatrix} \begin{bmatrix} V_p \\ V_{oc} \end{bmatrix} - \begin{bmatrix} R_0 + \frac{R_eR_p}{R_e+R_p} \end{bmatrix} i_t \quad (4)$$

III. SMOs for SoC Estimation

The SoC indicates the ratio of available capacity to the nominal capacity in the battery whose value changes between 0% and 100% [20]. According to the definition, the expression of SoC can be obtained through the current-time integral approach and it is given as

$$Z(t) = Z(0) - \frac{1}{Q_n}\int_{t_0}^{t} I(\tau)\eta(\tau)d\tau \quad (5)$$

where $Z(0)$ is the initial SoC, $I(\tau)$ is the instantaneous current which is assumed to be positive for discharging and the opposite for charging. The η is the columbic efficiency, which usually satisfies η=1 for discharging, and $\eta\leq$1 for charging for the batteries in the wide range of current and temperature [21]. The SMO has been widely used in the state estimation for its robustness and simplicity. The principle of SMO is that it feeds back the output estimated error via a switching function with a gain, the sliding mode term, which makes the system states move across the sliding mode surface and converges to the sliding mode surface

gradually [22]. The SMO has a common structure is shown in Fig. 3. $A \in R^{n\times n}$, $B \in R^{n\times 1}$, $C \in R^{1\times n}$, and $D \in R^{1\times 1}$ are coefficient matrixes which are composed of parameters of the battery. $u(t) \in R^{1\times 1}$ is a control variable, and $y \in R^{1\times 1}$ is the output voltage. The states estimation error is defined as $e(t) = x(t) - \hat{x}(t)$ and the output error is $e_y = y(t) - \hat{y}(t)$. The main difference in structures of SMO lies in the sliding mode term. The switching gain of the sliding mode term can be designed as a constant or as a variable related to the output error. According to the different designing of the switching gain, SMOs are classified into constant-gain SMO and adaptive-gain SMO. Then on the basis of order of the state equations, these methods are refined into first-order constant-gain SMO, second-order constant-gain SMO, and first-order adaptive-gain SMO.

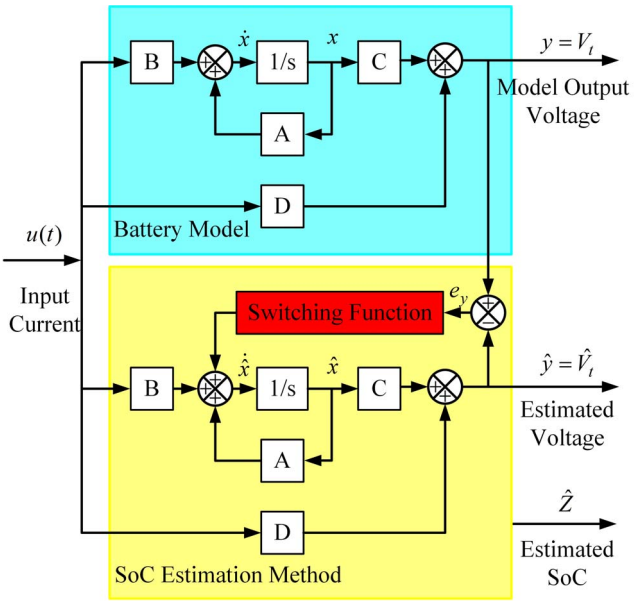

Fig. 3. General block diagram of the SMO method.

A. First-order Constant-Gain SMO

For the first-order constant-gain SMO, it can be expressed by first-order derivative equations of the state variable. [19], [23]-[25] designed the SMO based on three above ECMs respectively. They all have the same structure without Luenberger term:

$$\begin{aligned} \dot{\hat{x}}(t) &= A\hat{x}(t) + Bu(t) + L\,\mathrm{sign}(e) \\ \hat{y}(t) &= C\hat{x}(t) + Du(t) \end{aligned} \tag{6}$$

where the switching gain L are positive constants, the value of L depends on the design of the observer. The sign function is:

$$\mathrm{sign}(e) = \begin{cases} +1, & e > 0 \\ -1, & e < 0 \end{cases} \tag{7}$$

In the sliding mode term, independent variable e of the sign function is a vector containing different state errors. Taking [19] as an example, the RCCM is selected and the states are terminal voltage V_t, the state of charge Z and the voltage across the capacitance V_p. All elements of state error vectors $e = \begin{bmatrix} e_t & e_z & e_p \end{bmatrix}^T$ are $e_t = V_t - \hat{V}_t$, $e_z = Z - \hat{Z}$ and $e_p = V_p - \hat{V}_p$, respectively. According to the equivalent control method [19], the error system in sliding mode behaves as if $L\mathrm{sign}(e)$ is replaced by its equivalent value $\{L\mathrm{sign}(e)\}_{eq}$, which can be calculated assuming $\dot{e}_y = 0$ and $e_y = 0$. Using the same SMO structure as (6), [23] and [24] choose a first-order RCM while [25] a second-order RCM to establish the state-space function. On the other hand, a first-order RCM is employed and a Luenberger term is introduced to the sliding mode designing [26]. The structure of SMO is

$$\begin{aligned} \dot{\hat{x}}(t) &= A\hat{x}(t) + Bu(t) + K(y(t) - \hat{y}(t)) + L\,\mathrm{sign}(e_y) \\ \hat{y}(t) &= C\hat{x}(t) \end{aligned} \tag{8}$$

where $K = \begin{bmatrix} k_1 & k_2 & k_3 \end{bmatrix}^T$ is the Luenberger feedback gain, which is chosen so that the stability of the observer system is preserved. The error variable $e_y = y(t) - \hat{y}(t)$ is used as a feedback of each state function in the SMO.

In a control system which has any physical sense, high-frequency control switching may easily cause chattering effect. A possible solution is using continuous control to reduce the chattering effect [22]. Various kinds of anti-chattering functions are chosen in [27], [28] and [29] to substitute the sign function in [26]. An equivalent sign function $Eqv\,\mathrm{sign}(\cdot)$ is defined to reduce chattering levels [27] and it is defined as

$$Eqv\,\mathrm{sign}(e_y) = \frac{e_y}{|e_y| + \mu} \tag{9}$$

where μ is used to adjust the slope. Similarly, a saturation function $Sat(\cdot)$ is chosen in [28] and it is:

$$Sat(e_y) = \begin{cases} K_0 & e_y > K_0 \\ e_y & -K_0 < e_y < K_0 \\ -K_0 & e_y < -K_0 \end{cases} \tag{10}$$

In [29], the continuous anti-chattering function is implemented through the arc-tangent function $\tan^{-1}(e_y)$. A continuous hyperbolic tangent function is utilized in [21] and the function has the form of $\tanh a = \dfrac{e_y{}^a - e_y{}^{-a}}{e_y{}^a + e_y{}^{-a}}$.

B. Second-order Constant-Gain SMO

The structure of second-order SMO [30] for SoC estimation is:

$$\begin{aligned}
&\dot{\hat{x}}(t) = A\hat{x}(t) + Bu(t) + K(y(t) - \hat{y}(t)) + v_d(e_y) \\
&\dot{v}_d(e_y) = LSat\left(\frac{y(t) - \hat{y}(t)}{\phi}\right) \\
&\hat{y}(t) = C\hat{x}(t)
\end{aligned} \tag{11}$$

The sliding mode term not only consists of a Luenberger term with constant gain *K*, but also an integral term of the saturation function where ϕ determines the boundary layer. This kind of SMO has better performance in suppress switching ripple because the integral part can be regarded as a low pass filter and the saturation can suppress the ripple further. Hence it can drive to zero not only the sliding variable but also its derivative [22]. Another kind of second-order SMO is the super-twisting algorithm and it is applied to estimate SoC of the battery in [31]. The structure of super-twisting algorithms is

$$\begin{aligned}
&\dot{\hat{x}}(t) = A\hat{x}(t) + Bu(t) + Lv(e_y) \\
&v(e_y) = v_1(e_y) + v_2(e_y) \\
&v_1(e_y) = \lambda \left|e_y\right|^{\frac{1}{2}} \operatorname{sign}(e_y) \\
&\dot{v}_2(e_y) = \gamma \operatorname{sign}(e_y)
\end{aligned} \tag{12}$$

The super-twisting switching function is composed of two parts: one is a continuous function $v_1(e_y)$ and it guarantee that the system has quick response to reduce the error. The other is the time integral of sign function and it helps to eliminate the system error for the observed system.

C. First-order Adaptive-Gain SMO

Compared with the traditional first-order constant-gain SMO, the adaptive-gain SMO is able to dynamically adjust the switching gains in response to the tracking errors. It can guarantee the reachability of sliding mode surface and improve the SOC estimation accuracy further. Because of the good performance, this kind of SMO increasingly attracts researchers' attention. Based on the first-order RCM, the adaptive observer is designed as follows [32]:

$$\dot{\hat{x}}(t) = A\hat{x}(t) + Bu(t) + K(y(t) - \hat{y}(t)) + Bv \tag{13}$$

The control variable *v* is defined as

$$v = \begin{cases} -\rho \dfrac{\left(S^T MB\right)^T}{\left\|S^T MB\right\|^2} \|S\| \|MB\| & \left\|S^T MB\right\| \neq 0 \\ 0 & \left\|S^T MB\right\| = 0 \end{cases} \tag{14}$$

The design for the sliding mode surface is

$$S = F(\hat{y}(t) - y(t)) = FC(\hat{x}(t) - x(t)) = Me(t) = 0 \tag{15}$$

where *F* is the designed matrix, which makes the state variables in the surface slide to the zero equilibrium point, and $M = FC$. A similar observer is designed in [18] and there is another part added to the control variable *v* which is expressed as

$$v = \begin{cases} -\dfrac{\left(S^T MB\right)^T}{\left\|S^T MB\right\|^2}(\Delta_1 + \Delta_2) & \left\|S^T MB\right\| \neq 0 \\ 0 & \left\|S^T MB\right\| = 0 \end{cases} \tag{16}$$

where $\Delta_1 = \rho \|S\| \|MB\|$, $\Delta_2 = \eta(\frac{1}{2})^\beta \|S\|^{2\beta}$, $0 \le \eta \le 1$ and $\beta \ge 0$. Furthermore, [33] makes an improvement for the control variable *v* as follows:

$$v = \begin{cases} -\dfrac{\left(S^T M\right)^T}{\left\|S^T M\right\|^2}(\Delta_1 + \Delta_2) & \left\|S^T M\Gamma\right\| \neq 0 \\ 0 & \left\|S^T M\Gamma\right\| = 0 \end{cases} \tag{17}$$

where $\Delta_1 = \hat{\bar{\psi}} \|S\| \|M\Gamma\|$, $\Delta_2 = \eta(\frac{1}{2})^\beta \|S\|^{2\beta}$, $0 \le \eta \le 1$ and $\beta \ge 0$, $\hat{\bar{\psi}}$ is the upper bound of the system uncertainty. In [33], a radial basis function neural network is employed to adaptively learn an upper bound of system uncertainty. The switching gain is adjusted to adequate levels based on the learned upper bound to achieve asymptotic error convergence of the SOC estimation. [34]-[38] introduces another kind of adaptive sliding mode term and the switching gain is a function of e_y. The switching gain of SMO in [34] is the absolute value of e_y and the structure is as follows

$$\begin{aligned}
&\dot{\hat{x}}(t) = A\hat{x}(t) + Bu(t) + K(y(t) - \hat{y}(t)) + Lv \\
&v = \begin{cases} \left|e_y\right| \operatorname{sign}(e_y) & e_y(t) \neq 0 \\ 0 & e_y(t) = 0 \end{cases}
\end{aligned} \tag{18}$$

In addition, [35] uses $\sqrt{\left|e_y\right|}$ to substitute the $\left|e_y\right|$ in the above control variable *v*. Similarly, a linear function of $\sqrt{\left|e_y\right|}$ is adopted in [36] where the sliding mode term was designed as:

$$L_i \operatorname{sign}(e_i) = \begin{cases} \left(\delta_i + k_i \sqrt{\left|e_y\right|}\right) \operatorname{sign}(e_i(t)) & e_i(t) \neq 0 \\ 0 & e_i(t) = 0 \end{cases} \tag{19}$$

where e_i is the *i-th* state estimation error. Integral of output error e_y is used to be the sliding mode gain, which makes the gain auto-turning in [37].

TABLE I. PERFORMANCE COMPARISON AMONG VARIOUS SMOS

Methods	Sliding mode term	Simply design	Accuracy	Anti-chattering
first-order constant gain SMO	$v=\text{sign}(e)$	++[a]	+	+
Second-order constant gain SMO	$v=\text{sign}(e)+\int \text{sign}(e)dt$	+	++	++
First-order adaptive gain SMO	$v=f(e)\text{sign}(e)$	+	++	++

[a] +: good, ++: better

SMOs have the structure of $\dot{\hat{x}}(t)=A\hat{x}(t)+Bu(t)+K(y(t)-\hat{y}(t))+Lv$, and v is the sliding mode term.

$$L_i\text{sign}(e_i)=\begin{cases}\int\left(\gamma_i|e_i|\right)dt\times\text{sign}(e_i(t)) & e_i(t)\neq 0\\ 0 & e_i(t)=0\end{cases} \quad (20)$$

By means of the equivalent control method [19], $L\text{sign}(e)$ can be replaced by its equivalent value $\{L\text{sign}(e)\}_{eq}$. For simplification, adaptive switching gain was designed as the integral of e_y in [38], therefore the following adaptive sliding mode term was obtained.

$$L\text{sign}(e_y)=\begin{cases}\int\left(\gamma|e_y|\right)d\times\text{sign}(e_y) & e_y(t)\neq 0\\ 0 & e_y(t)=0\end{cases} \quad (21)$$

D. Comparison

In order to compare the performance of above SMOs, the simplicity of design, estimation accuracy, anti-chattering are considered, forming a performance comparison table I. Each cell in this table contains symbols + or ++, indicating that the performance related to that column is good or better among these SMO methods. As shown in Table I, the design process of conventional first-order constant-gain SMO is simple, but the estimation accuracy is comparative low. Because the high frequency switching ripple is introduced into the feedback loop as a result of switching function. Second-order constant-gain SMO is a desired choice to suppress ripple, because it adds an integral term of the sign function behaving as a low-pass filter. Under this condition, both the error and its derivative between the actual state and estimated state can converge to zero. As a result, the accuracy is improved but the design of sliding mode gain is more difficult than the former SMO. The principle of the first-order adaptive-gain SMO is to adaptively tune the sliding mode gain online, and therefore the chattering is suppressed. Similarly, the design process is also complex. According to existing literatures, there is not a comparative study between the latter two SMOs. In this paper, the performance of them is considered temporarily same and the problem that which kind of SMO is better is still worth to be researched.

IV. CONCLUSION

This paper investigates various SMO methods based on ECM for battery SoC estimation and classifies them into first-order constant gain SMO, second-order constant gain SMO, and first-order adaptive gain SMO. By discussing the principles of different SMO algorithms, the pros and cons of these methods are compared. Conventional first-order constant gain SMO is simply designed and easy to implement, however, the switching functions will cause high frequency chattering phenomenon. Continuous control is a possible solution to reduce the chattering effect, therefore various anti-chattering functions are chosen to substitute the sign function. Second-order SMO is also an important technique to achieve continuous control. It introduces an integral term into switching function which can guarantee the sliding variable and its derivative converge to zero in finite time. As a consequence, the chattering effect can be significantly reduced. In addition, first-order adaptive SMO also can suppress the switching ripple and guarantee good estimation accuracy. But it is not sure which case of observer is better for second-order SMO and first-order adaptive SMO.

REFERENCES

[1] B. Bilgin, P. Magne, P. Malysz, Y. Yang, V. Pantelic, M. Preindl, A. Korobkine, W. Jiang, M. Lawford and A. Emadi, "Making the case for electrified transportation," IEEE Trans. Transport. Electrif., vol. 1, no. 1, pp. 4-17, 2015.

[2] M.A. Hannan, M.H. Lipu, A. Hussain and A. Mohamed, "A review of lithium-ion battery state of charge estimation and management system in electric vehicle applications: Challenges and recommendations," Renew. Sust. Energ. Rev, vol. 78, pp. 834-854, 2017.

[3] M.U. Cuma and T. Koroglu, "A comprehensive review on estimation strategies used in hybrid and battery electric vehicles," Renew. Sust. Energ. Rev., vol. 42, pp. 517-531, 2015.

[4] W. Waag, C. Fleischer and D.U. Sauer, "Critical review of the methods for monitoring of lithium-ion batteries in electric and hybrid vehicles," J. Power Sources, vol. 258, pp. 321-339, 2014.

[5] J. Meng, M. Ricco, A.B. Acharya, G. Luo, M. Swierczynski, D. Stroe and R. Teodorescu, "Low-complexity online estimation for LiFePO 4 battery state of charge in electric vehicles," J. Power Sources, vol. 395, pp. 280-288, 2018.

[6] J. Meng, G. Luo and F. Gao, "Lithium polymer battery state-of-charge estimation based on adaptive unscented kalman filter and support vector machine," IEEE Trans. Power Electron, vol. 31, no. 3, pp. 2226-2238, 2016.

[7] Q. Wang, Y. He, J. Shen, X. Hu and Z. Ma, "State of charge-dependent polynomial equivalent circuit modeling for electrochemical impedance spectroscopy of lithium-ion batteries," IEEE Trans. Power Electron., vol. 33, no. 10, pp. 8449-8460, 2018.

[8] B. Pattipati, C. Sankavaram and K. Pattipati, "System identification and estimation framework for pivotal automotive battery management system characteristics," IEEE Trans. on Syst. Man, Cybern. C, Appl. Rev., vol. 41, no. 6, pp. 869-884, 2011.

[9] J. Chen, Q. Ouyang, C. Xu and H. Su, "Neural network-based state of charge observer design for lithium-ion batteries," IEEE Trans. Control Syst. Technol., vol. 26, no. 1, pp. 313-320, 2018.

[10] J. Wu, Y. Wang, X. Zhang, and Z. Chen, "A novel state of health estimation method of Li-ion battery using group method of data handling," J. Power Sources, vol. 327, pp. 457–464, 2016.

[11] J. C. Alvarez Anton, P. J. Garcia Nieto, C. Blanco Viejo, and J. A. Vilan, "Support vector machines used to estimate the battery state of charge," IEEE Trans. Power Electron., vol. 28, no. 12, pp. 5919–5926, 2013.

[12] J. Du, Z. Liu, and Y. Wang, "State of charge estimation for Li-ion battery based on model from extreme learning machine," Control Eng. Pract., vol. 26, no. 1, pp. 11–19, 2014

[13] P. Shen, M. Ouyang, L. Lu, J. Li and X. Feng, "The co-estimation of state of charge, state of health, and state of function for lithium-ion batteries in electric vehicles," IEEE Trans. Veh. Technol., vol. 67, no. 1, pp. 92-103, 2018.

[14] Q. Zhu, L. Li, X. Hu, N. Xiong and G. Hu, "H∞-based nonlinear observer design for state of charge estimation of lithium-ion battery with polynomial parameters," IEEE Trans. Veh. Technol., vol. 66, no. 12, pp. 10853-10865, 2017.

[15] X. Liu, Z. Chen, C. Zhang and J. Wu, "A novel temperature-compensated model for power li-ion batteries with dual-particle-filter state of charge estimation," Appl. Energy, vol. 123, pp. 263-272, 2014.

[16] J. K. Barillas, J. Li, C. Günther and M.A. Danzer, "A comparative study and validation of state estimation algorithms for li-ion batteries in battery management systems," Appl. Energy, vol. 155, pp. 455-462, 2015.

[17] X. Hu, S. Li, and H. Peng, "A comparative study of equivalent circuit models for Li-ion batteries," J. Power Sources, vol. 198, pp. 359–367, 2012.

[18] Q. Chen, J. Jiang, H. Ruan, and C. Zhang, "Simply designed and universal sliding mode observer for the SOC estimation of lithium-ion batteries," IET Power Electron., vol. 10, no. 6, pp. 697–705, 2017.

[19] I. S. Kim, "Nonlinear state of charge estimator for hybrid electric vehicle battery," IEEE Trans. Power Electron., vol. 23, no. 4, pp. 2027–2034, 2008.

[20] J. Meng, M. Ricco, G. Luo, M. Swierczynski, D.-I. Stroe, and R. Teodorescu, "An overview and comparison of online implementable SOC estimation methods for Lithium-ion battery," IEEE Trans. Ind. Appl., vol. 54, no. 2, pp. 1583-1591, 2018.

[21] Q. Ouyang, J. Chen, J. Zheng, and Y. Hong, "SOC estimation-based quasi-sliding mode control for cell balancing in lithium-ion battery packs," IEEE Trans. Ind. Electron., vol. 65, no. 4, pp. 3427–3436, 2018.

[22] Y. Shtessel, C. Edwards, L. Fridman, A. Levant, Sliding Mode Control and Observation, Boston, MA, USA:Birkhäuser, 2013.

[23] B. Ning, B. Cao, B. Wang, and Z. Zou, "Adaptive sliding mode observers for lithium-ion battery state estimation based on parameters identified online," Energy, vol. 153, pp. 732–742, 2018.

[24] B. Xiong, J. Zhao, Y. Su, Z. Wei, and M. Skyllas-Kazacos, "State of charge estimation of vanadium redox flow battery based on sliding mode observer and dynamic model including capacity fading factor," IEEE Trans. Sustain. Energy, vol. 8, no. 4, pp. 1658–1667, 2017.

[25] X. Chen, W. X. Shen, Z. Cao, and A. Kapoor, "Sliding mode observer for state of charge estimation based on battery equivalent circuit in electric vehicles," Aust. J. Electr. Electron. Eng., vol. 9, no. 3, pp. 225–234, 2015.

[26] I. S. Kim, "The novel state of charge estimation method for lithium battery using sliding mode observer," J. Power Sources, vol. 163, no. 1, pp. 584–590, 2006.

[27] J. Mao, L. Zhao, and Y. Lin, "State-of-charge estimation of lithium-ion polymer battery based on sliding mode observer," in Proc. 33rd Chinese Control Conf.(CCC), pp. 269–273, 2014.

[28] T. Kim, W. Qiao, and L. Qu, "Online SOC and SOH estimation for multicell lithium-ion batteries based on an adaptive hybrid battery model and sliding-mode observer," 2013 IEEE Energy Convers. Congr. Expo. (ECCE), pp. 292–298, 2013.

[29] G. Vicidomini, G. Petrone, E. Monmasson, and G. Spagnuolo, "FPGA based implementation of a slding-mode observer for battery state of charge estimation," IEEE 26th Int. Symp. Ind. Electron. (ISIE), pp. 1268–1273, 2017.

[30] D. Kim, K. Koo, J. J. Jeong, T. Goh, and S. W. Kim, "Second-order discrete-time sliding mode observer for state of charge determination based on a dynamic resistance li-ion battery model," Energies, vol. 6, no. 10, pp. 5538–5551, 2013.

[31] Y. Huangfu, J. Xu, D. Zhao, Y. Liu, and F. Gao, "A novel battery state of charge estimation method based on a super-twisting sliding mode observer," Energies, vol. 11, no. 5, pp. 1211, 2018.

[32] Q. Chen, J. Jiang, H. Ruan, and C. Zhang, "A new double sliding mode observer for EV lithium battery SOC estimation," Math. Probl. Eng., vol. 2016, pp. 1-9, 2016.

[33] X. Chen, W. Shen, M. Dai, Z. Cao, J. Jin, and A. Kapoor, "Robust adaptive sliding-mode observer using RBF neural network for lithium-ion battery state of charge estimation in electric vehicles," IEEE Trans. Veh. Technol., vol. 65, no. 4, pp. 1936–1947, 2016.

[34] Y. Tian, B. Xia, M. Wang, W. Sun, and Z. Xu, "Comparison study on two model-based adaptive algorithms for SOC estimation of lithium-ion batteries in electric vehicles," Energies, vol. 7, no. 12, pp. 8446–8464, 2014.

[35] Y. G. Huangfu, J. N. Xu, S. R. Zhuo, M. C. Xie, and Y. T. Liu, "A novel adaptive sliding mode observer for SOC estimation of lithium batteries in electric vehicles," 7th Int. Conf. Power Electron. Syst. Appl. - Smart Mobility, Power Transf. Secur. (PESA), pp. 1–6, 2017.

[36] W. Chunyu, C. Naxin, L. Miao, and Z. Chenghui, "A new State of charge estimation method for lithium-ion battery based on sliding mode observer," IEEE Energy Convers. Congr. Expo. (ECCE), pp. 5625–5630, 2017.

[37] X. Chen, W. Shen, Z. Cao, and A. Kapoor, "Adaptive gain sliding mode observer for state of charge estimation based on combined battery equivalent circuit model," Comput. Chem. Eng., vol. 64, pp. 114–123, 2014.

[38] X. Chen, W. Shen, Z. Cao, and A. Kapoor, "A novel approach for state of charge estimation based on adaptive switching gain sliding mode observer in electric vehicles," J. Power Sources, vol. 246, pp. 667–678, 2014.